EPJ Web of Conferences **2**, 04005 (2010)
DOI:10.1051/epjconf/20100204005

Combinatorial level densities for practical applications

S. Hilaire[1,a], S. Goriely[2], M. Girod[1], A. J. Koning[3], R. Capote[4], and M. Sin[5]

[1] CEA, DAM, DIF, F-91297, Arpajon, France
[2] Institut d'Astronomie et d'Astrophysique, Université Libre de Bruxelles, Campus de la Plaine CP 226, BE-1050 Brussels, Belgium
[3] Nuclear Research and Consultancy Group, P.O. Box 25, NL-1755 ZG Petten, The Netherlands
[4] Nuclear Data Section, International Atomic Energy Agency, Wagramerstrasse 5, Vienna AT-1400, Austria
[5] Nuclear Physics Department, Bucharest University, Bucharest-Magurele, Romania

Abstract. We review our calculated energy-, spin- and parity-dependent nuclear level densities based on the microscopic combinatorial model described in ref. [1]. We show that this model predicts the experimental s- and p-wave neutron resonance spacings with a degree of accuracy comparable to that of the best global models available and also provides reasonable description of low energies cumulative number of levels as well as of the experimental data obtained by the Oslo group [2]. We also provide a renormalization recipe which enables to play with the tabulated results for practical applications. Finally, we study the impact of temperature dependent calculation on s-wave neutron resonance spacings.

1 Introduction

The knowledge of nuclear level densities (NLDs) has been a matter of interest and study for years going back at least to 1936 with Bethe's pioneering work [3]. Level densities are required when modeling nuclear reactions as soon as the number of levels to which decay occurs is too large to allow for an individual description. With the development of new industrial or experimental facilities, as well as for astrophysical interest, the increasing need of nuclear data far from the valley of stability challenges the nuclear reaction models. Indeed, so far, cross section predictions have relied on more or less phenomenological approaches, depending on parameters adjusted to scarce experimental data or deduced from systematical relations. While such predictions are expected to remain reliable for nuclei not too far from experimentally accessible regions, the predictive power of analytical models in general, and of analytical level densities expressions in particular, is more and more questionable when dealing with more and more exotic nuclei. To face such difficulties, it is preferable to rely on approaches as fundamental as possible. Such microscopic description by a physically sound model based on first principles ensures a reliable extrapolation away from experimentally known region.

Global microscopic models of NLD have been developed for the last decades (see [1] and references therein), but they have almost never been used for practical applications, because of their lack of accuracy in reproducing experimental data (especially when considered globally on a large data set) or because they do not offer the same flexibility as that of the highly parametrized analytical expressions. We have therefore developed a combinatorial approach and demonstrated that such an approach can clearly compete with the statistical approach in the global reproduction of experimental data [1,4]. As we will see, this approach provides the energy, spin and parity dependence of the NLD, and, at low energies, describes the non-statistical limit which, by definition cannot be described by statistical-based analytical approaches, and yet clearly can have a significant impact on cross section predictions. We will also show how we plan to improve our predictions in the coming future.

2 The combinatorial method

The combinatorial method has been extensively described in refs. [1,4,5] and we just summarize here its main features. It consists in using the single-particle level schemes obtained from constrained axially symmetric Hartree-Fock-Bogoliubov (HFB) method based on the BSk14 Skyrme force [6] to construct incoherent particle-hole (ph) state densities as a function of the excitation energy, the spin projection (on the intrinsic symmetry axis of the nucleus) and the parity. Once these incoherent ph state densities are determined, collective effects are included. In [4] the vibrational effects was described by multiplying the total level densities by a phenomenological enhancement factor similar to that of refs.[7,8] once rotational bands had been constructed. However, such a choice has shown its limits [9] and has been replaced by an improved but more complicated treatment. The latter explicitly allows for phonon excitations using the boson partition function of ref. [5] and includes quadrupole, octupole as well as hexadecapole vi-

[a] e-mail: stephane.hilaire@cea.fr

brational modes. However, whereas single-particle levels are theoretically obtained for any nucleus, phonon's energies are taken from experimental information when available and from analytical expressions [1] otherwise. Once the vibrational and incoherent ph state densities are computed, they are folded to deduce the total state densities. Level densities are then obtained by constructing rotational bands if present (i.e. if the nucleus is deformed) or using the classical expression that relates state and level densities for a spherical nucleus [1]. To account for the damping of vibrational effects with increasing energies, we restrict the folding to the ph configurations having a total exciton number (i.e. the sum of the number of proton and neutron particles and proton and neutron holes) $N_{ph} \leq 4$. This restriction stems from the fact that a vibrational state results from a coherent excitation of particles and holes, and that this coherence vanishes with increasing number of ph involved in the description. Therefore, if one deals with a ph configuration having a large exciton number, one should not simultaneously account for vibrational states which are clearly already included as incoherent excitations.

3 Results

The new NLD are now compared with experimental data. In spite of considerable experimental efforts made to derive NLD, the lack of reliable data–especially over a wide energy range–constitutes the main problem that the NLD theories have to face. Nevertheless, a large number of analysis of slow neutron resonances and of cumulative numbers of low energy levels have greatly helped to provide experimental information on NLD. Other sources of information have also been suggested, such as analysis of spectra of evaporated particles and coherence widths of cross section fluctuations. However, most of these experimental data are affected by systematic errors resulting from experimental uncertainties as well as the use of approximate theories to analyze them.

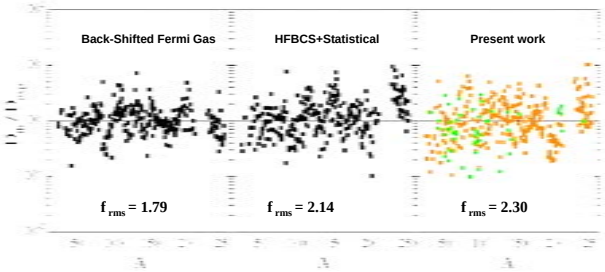

Fig. 1. Ratio of HFB plus combinatorial (D_{th}) to the experimental (D_{exp}) s-wave (squares) and p-wave (circles) neutron resonance spacings compiled in [10] compared with other global approaches such as the Back-Shifted-Fermi-Gas model of ref. [11] and the HFBCS+statistical approach of ref. [12].

The most extensive and reliable source of experimental information on NLD remains the s-and p-wave neutron resonance spacings [8,10] and the observed low-energy excited levels [10]. We show in Fig. 1 the result of our HFB plus combinatorial approach with respect to experimental s- and p-wave spacings compiled in the RIPL-2 database [10]. The quality of a global NLD formula can be described by the rms deviation factor defined as

$$f_{rms} = \exp\left[\frac{1}{N_e}\sum_{i=1}^{N_e} \ln^2 \frac{D^i_{th}}{D^i_{exp}}\right]^{1/2}, \qquad (1)$$

where $D_{th}(D_{exp})$ is the theoretical (experimental) resonance spacing and N_e is the number of nuclei in the compilation. Globally, as can be seen in Fig. 1, the resonance spacings are predicted within a factor of 2 (the exact rms factor amounts to $f_{rms} = 2.3$) for both the s- and p-wave data. This result is to be compared to the deviations of global analytical formula [11,13] typically of the order of $1.7 - 1.9$ and to the $f_{rms} = 2.14$ value obtained with the HFBCS+statistical model introduced in ref. [12], which was the first global microscopic NLD prescription having the capacity to compete with phenomenological models in the reproduction of experimental data. Our new approach therefore gives rather comparable predictions with respect to the other existing global models.

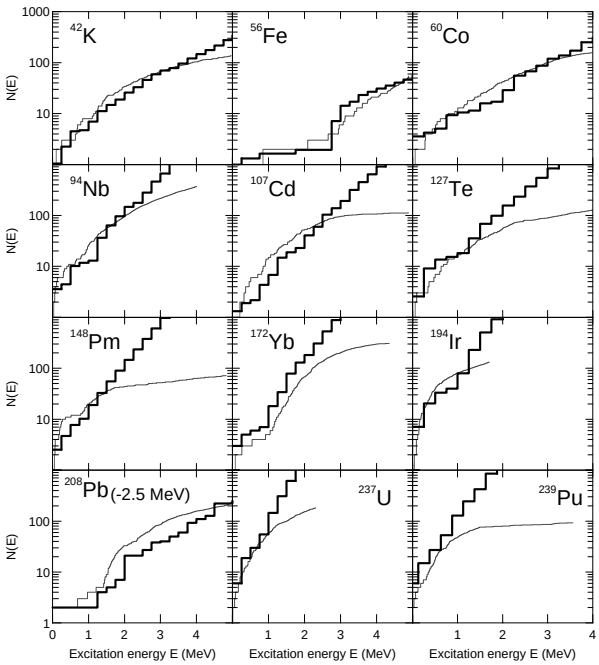

Fig. 2. Comparison of the cumulative number of observed levels (thin staircase) with the HFB plus combinatorial predictions (thick line) as a function of the excitation energy U for a sample of 12 nuclei. Only for ^{208}Pb, both curves have been shifted by 2.5 MeV, the energy range corresponding consequently to [2.5-7.5] MeV instead of [0-5] MeV.

The HFB plus combinatorial model also gives satisfactory extrapolations to low energies. As an example, we

compare in Fig. 2 the predicted cumulative number of levels $N(U)$ with the experimental data [10] for 12 nuclei, including light as well as heavy and spherical as well as deformed species. Globally, the present model provides similar results as those illustrated in Ref.[4]. Yet one can observe significant disagreement in certain case which could be reduced with a simple renormalization procedure. Such renormalizations are also often required, in particular for nuclear data evaluation or for an accurate and reliable estimate of reaction cross sections. Though the HFB plus combinatorial NLD are provided in a table format, it is possible to renormalize them on both the experimental level scheme at low energy and the neutron resonance spacings at $U = S_n$ in a way similar to what is usually done with analytical formulae. More specifically, the level density can be renormalized through the expression

$$\rho(U,J,P)_{renorm} = e^{\alpha\sqrt{(U-\delta)}} \times \rho(U-\delta,J,P) \qquad (2)$$

where the energy shift δ is essentially extracted from the analysis of the cumulative number of levels and α from the experimental s-wave neutron spacing. With such a renormalization, the experimental low-lying levels and the D_{exp} values can be reproduced reasonably well, as discussed in detail in [13]. Eq.(2) has been used to fit the 289 nuclei for which both an experimental s-wave spacing (D_0) and a discrete level sequence exist. The corresponding δ and α values are plotted in Fig. 3. It is important to note that the obtained α and δ parameters show no systematic trend or A-dependence, and more particularly no correlation with shell closures. Of course, when no D_{exp} value is available and only the experimental discrete level scheme is known, only the δ shift is used to reproduce at best the low-lying levels.

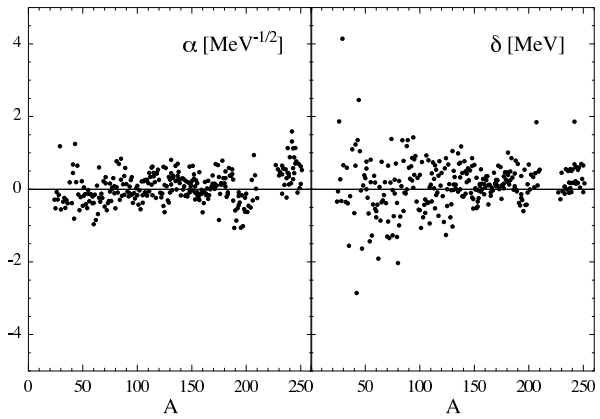

Fig. 3. α and δ values plotted as a function of the atomic mass. See text for more details.

Comparisons have also been performed with the experimental data extracted by the Oslo group from the analysis of particle-γ coincidence in the (^{3}He,$\alpha\gamma$) and (^{3}He,^{3}He'γ) reactions [2]. The experimental determination of level densities out of these reactions is however model-dependent and requires a normalization at the neutron binding energy as explained and discussed in ref. [1]. If we normalize our calculation using the same total level density as that of the Oslo group, using Eq. (2) for each isotope, with an α parameter such that

$$\rho_{\rm HFB}(S_n) \times \exp(\alpha\sqrt{S_n}) = \rho_{\rm oslo}(S_n) \qquad (3)$$

our combinatorial results agree extremely well with the so-called experimental values below S_n, as illustrated in Fig. 4.

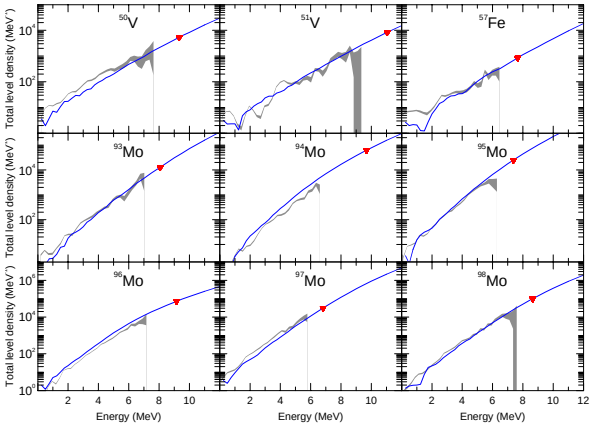

Fig. 4. Comparison between the total NLD determined by the Oslo group (Grey areas) and the HFB combinatorial predictions (solid lines). The full triangles correspond to the model-dependent normalization point derived from the D_0 value used by the Oslo group. See text for more details.

As mentioned previously, one advantage of the combinatorial method with respect to the statistical method is its non statistical feature which enables us to obtain realistic parity and spin distributions. Deviations from the usually adopted equipartition of parities have been shown to have a non negligible impact, in particular when looking at capture cross sections [4]. Concerning the spin distribution, the combinatorial approach provides nuclear level densities which strongly deviate from the usually adopted Wigner law, in particular at low energy. Such deviations can play a key role in the description of the decay to spin isomers at low energies [14], since high spin population is usually strongly underestimated within a statistical approach. In particular, this implies an underestimate of the decaying probability to high spin levels.

Last but not least, is the test of our predictions in the most complicated case of fission cross section predictions. Indeed, one has then to deal with nuclear reactions, which involve not only the level densities at equilibrium deformations but also at deformation corresponding to the top of each fission barrier encountered in the classical modeling of the fission process in terms of multiple humped fission barriers. If very accurate fits of fission cross section can be achieved [15,16], it is mainly thanks to the use of

a very large number of parameters which are generally not constrained by experimental data. More than in any other channel, the predictive power of the traditional approaches is poor, and by no mean such approaches can be employed to make extrapolations far from the regions where fission cross section has been measured. The only solution left in this case is to rely on microscopic predictions provided they give reasonable answers. Quite a complete study has been performed on the use of microscopic ingredients applied to fission cross section prediction [17] and we just summarize here part of this work, by plotting in Fig. 5, calculated fission cross sections using both the microscopic fission barriers and associated combinatorial level densities for several actinides. As can be seen, the quality ob-

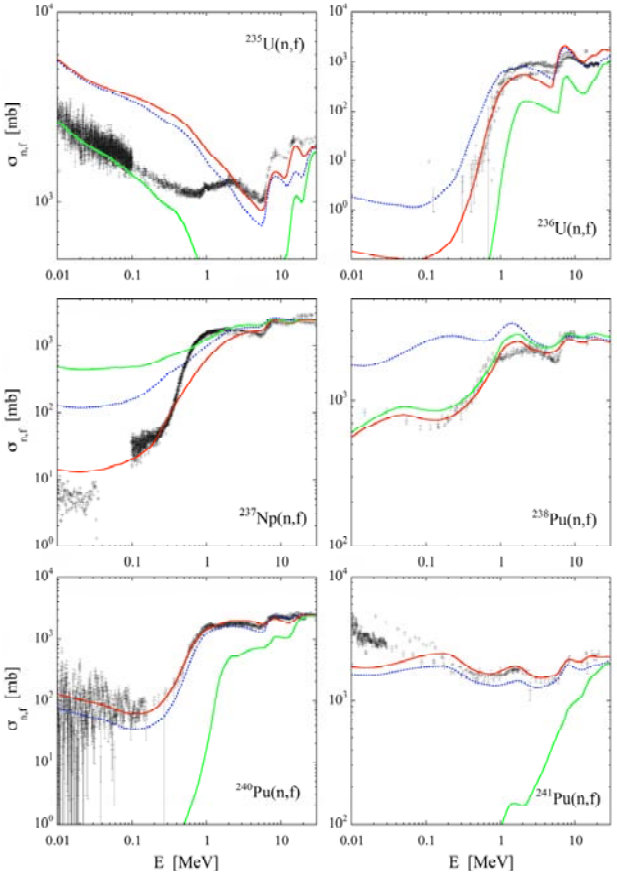

Fig. 5. Neutron-induced fission cross sections obtained with the microscopic fission path and the combinatorial nuclear level densities using the raw fission paths (green lines), when the fission paths are renormalized for each actinide (red line) or by a systematical factor depending on the oddness of the nuclei (blue dotted line).

tained by default (green line) is not satisfactory for practical applications which require a few percent of accuracy. In this case both nuclear level densities and fission barriers are directly obtained from HFB+BSk14 predictions. The bad description obtained using these raw (not adjusted) ingredients is mainly due to the fact that the microscopic barriers are generally too high by a few hundreds of keV [6, 17] which is too big an error to provide reasonable cross sections. If the barriers are individually normalized, without even modifying the combinatorial level densities, it is possible to obtain cross sections which are in much better agreement with experimental data (red lines). However, such normalizations only make sense if experimental data are available. If not, it is still possible to use systematic normalizations deduced by averaging those which have been obtained fitting the nuclei for which experimental data are available. In that case, one obtains fission cross section which are globally within a factor of 3 (blue dotted lines). Of course, the quality of the fit can be further improved using Eq. 2, but this would go beyond our present discussion.

4 Temperature effect on combinatorial level densities

We have seen that the combinatorial level densities we have obtained and tabulated provide quite good results when compared to available experimental data as well as when they are used to produce cross sections, even in complicated reactions such as neutron induced fission on actinides. Yet, they still suffer from several approximations which can be reduced with more or less complicated treatment. Among these approximations, the way collective enhancement evolves with increasing excitation energy remains questionable. If it is well established that with increasing energy, a deformed nucleus in its ground state becomes spherical and that the vibrational enhancement vanishes. These features are usually described using more or less elaborated phenomenological approximations [12, 18]. The disappearance of the rotational enhancement at increasing excitation energies has already been studied theoretically [19] for a few nuclei but not within a systematic approach. Another way to describe this transition to sphericity is to use temperature-dependent HFB approach following the method described in ref. [20]. In particular, for a heated system, the average value of an observable O reads

$$\bar{O} = \frac{\int O \exp[-F(q)/T] dq}{\int \exp[-F(q)/T] dq} \qquad (4)$$

where the free energy F depends on the energy E, the temperature T and the entropy S through the usual relation $F(q) = E(q) - TS(q)$ and q is the quadrupole deformation considered to be the most relevant property to describe the deformation changes with the temperature evolution. In a first approximation, neglecting the thermal fluctuation, the equilibrium deformation of the nucleus at a temperature T corresponds to the one minimizing the free energy F. For a given temperature, corresponding to a given excitation energy $U = E - E(T = 0)$, the single-particle level scheme and pairing properties have been determined at the equilibrium deformation to estimate the level density on the basis of our combinatorial method. The recently determined D1M Gogny force [21] is used here to estimate all nuclear ingredients. As illustrated in Fig. 6, the obtained level den-

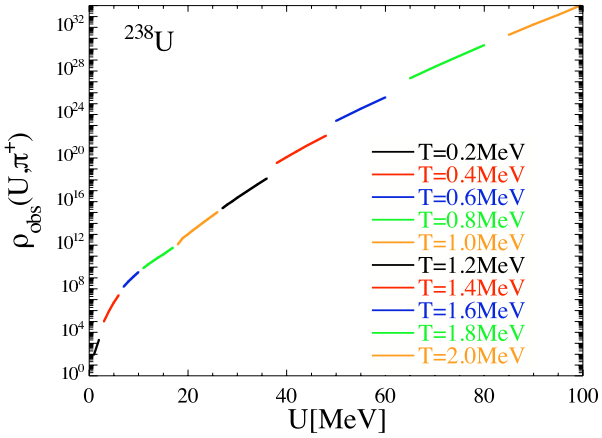

Fig. 6. Total nuclear level densities for ^{238}U calculated for several temperatures. Each level density curve covers an energy interval which starts at the excitation energy corresponding to the chosen temperature. In the present case the total level density is plotted without any smoothing procedure (see text for more details).

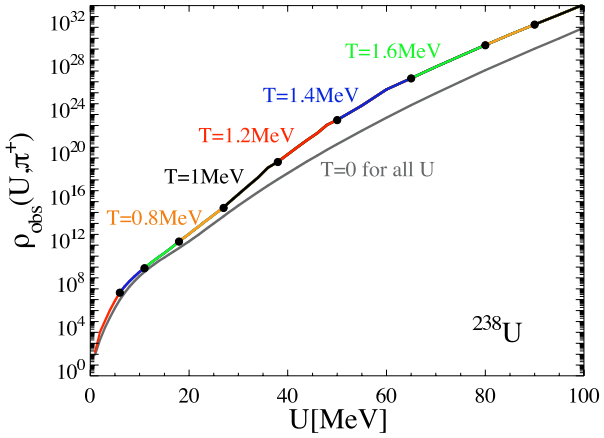

Fig. 7. Total nuclear level densities for ^{238}U calculated for several temperatures connected smoothly thanks to the procedure described in the text. The reference points, i.e those not affected by the smoothing procedure, are also plotted. The level density obtained using the HFB ingredients determined with $T = 0$ is shown for comparison (gray curve).

sities strongly depend on the corresponding temperature and display discontinuities stemming from the vanishing (gradual or sudden) of shell and pairing effects as well as from the fact that we use a finite set of temperatures to compute our level densities. Indeed, in principle the level density determined for a given temperature is only valid at the corresponding excitation energy. However, for practical reasons, we consider the level density determine for the temperature T_i to be valid over the excitation energy interval $[U_i, U_{i+1}]$. To suppress the discontinuity at a given temperature T_i, an energy-dependent shift is applied to the level density in the $[U_{i-1}, U_i]$ range. With such a simple treatment, the discontinuous level density of Fig. 6 can be regularized into that illustrated in Fig. 7 and the NLD estimated within a reasonable computer time.

As can observed, the temperature dependent level density is significantly different from that obtained on the basis of the $T = 0$ ingredients. In particular, the T-dependent HFB plus combinatorial NLD is higher than the one obtained with the $T = 0$ approximation, stemming from a modification of the single-particle configuration at increasing energies and in particular the disappearance of the shell effect. The temperature effect has a non negligible impact even at low energies around the neutron binding energy and consequently may affect the prediction of the s-wave spacing at B_n. To check that, we have estimated the T-dependent HFB plus combinatorial NLD for all the nuclei for which an experimental s-wave spacing is available. The results are displayed in Fig. 8 and compared with the results obtained within the $T =$ approximation. The improvement obtained with the temperature dependent method is quite clear. In terms of the to f_{rms} factor introduced in Eq.(1), we found $f_{rms} = 4$ in the $T = 0$ case and $f_{rms} = 2.7$ for the temperature-dependent calculation. Note however that contrary to what has been done in ref. [1], we have not included here any hexadecapole vibrational phonon the energy of which remains highly uncer-

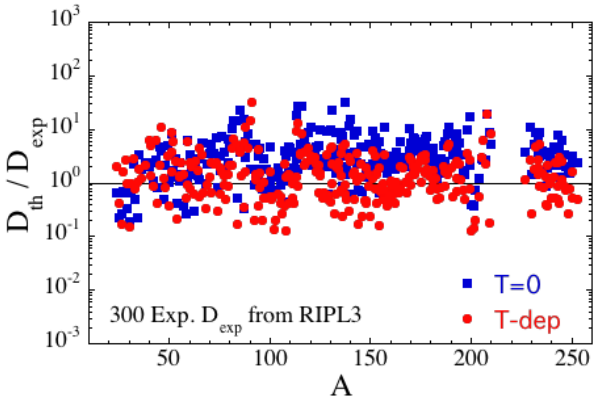

Fig. 8. Ratio of HFB plus combinatorial (D_{th}) to the experimental (D_{exp}) s-wave neutron resonance spacings compiled in [10] with the temperature dependent treatment (red circles) and using the HFB ingredients obtained for $T = 0$ (squares).

tain. In the current situation, the only phenomenological ingredients are the octupole vibrational phonon energies and the number of phonons and particle-hole configuration included in the vibrational-intrinsic state density folding procedure. In particular note that the analytical expression for the quadrupole phonons' energies has now been replaced by those predicted coherently using the method described in refs. [22,23] on the basis of the same D1M Gogny interaction [21].

5 Conclusion

Microscopic nuclear level densities have been determined for more than 8000 nuclei in a tabular form using the combinatorial method. These tables are available at the website *http://www-astro.ulb.ac.be* and we have shown they pro-

vide fairly good results both when compared with purely experimental level density data or when employed to predict nuclear reaction cross sections. Yet, the combinatorial method can still be improved to better account for collective effects and in particular their evolution with excitation energy. A first attempt has been made to account for the variations of nuclear structure properties with increasing excitation energy through the temperature-dependent Hartree-Fock-Bogoliubov calculations. The results are very promising and encouraging for further investigation.

References

1. S. Goriely, S. Hilaire, and A. J. Koning, Phys. Rev. C **78**, (2008) 064307.
2. A.C. Larsen et al., Phys. Rev. C **73**, (2006) 064301 and references therein.
3. H.A. Bethe, Phys. Rev. **50**, (1936) 332.
4. S. Hilaire and S. Goriely, Nucl. Phys. A **779**, (2006) 63.
5. S. Hilaire, J.P. Delaroche and M. Girod, Eur. Phys. J. A **12**, (2001) 169.
6. S. Goriely, M. Samyn, and J. M. Pearson, Phys. Rev. C **75**, (2007) 064312.
7. A.V. Ignatyuk, IAEA report, INDC(CCP)-233/L (1985).
8. A.V. Ignatyuk, IAEA report, TECDOC-1034, (1998).
9. M. Sin et al., *Nuclear Data for Science and Technology* O. Bersillon et al (eds); EDP Sciences, (2008) p. 313.
10. Belgya T., Bersillon, O., Capote Noy, R. et al., *Handbook for calculations of nuclear reaction data, RIPL-2* (IAEA-Tecdoc-1506), 2006.
11. S. Goriely et al., J. Nucl. Sci. Technol. Suppl. **2**, (2002) 536.
12. P. Demetriou and S. Goriely, Nucl. Phys. A **695**, (2001) 95.
13. A.J. Koning, S. Hilaire, S. Goriely, Nucl. Phys. **A810**, 13 (2008).
14. S. Goko et al., Phys. Rev. Lett. **96**, (2006) 192501.
15. M. Sin et al., Phys. Rev. C **74** (2006) 014608.
16. M.J. Lopéz Jiménez et al., Ann. Nucl. Energy **32** (2005) 195.
17. S. Goriely et al., Phys. Rev. C. **79**, (2009) 024612.
18. A.R. Junghans et al., Nucl. Phys. A **629**, (1998) 635.
19. G. Hansen and A.S. Jensen, Nucl. Phys. A **406**, (1983) 236.
20. V. Martin, J.L. Egido and L.M. Robledo, Phys. Rev. C **68**, (2008) 034327.
21. S. Goriely et al., Phys. Rev. Lett. **102**, (2009) 242501.
22. G. F. Bertsch et al., Phys. Rev. Lett. **99**, (2007) 032502.
23. J. P. Delaroche et al., submitted to Phys. Rev. C.